

# GET-Zero: Graph Embodiment Transformer for Zero-shot Embodiment Generalization

Austin Patel      Shuran Song

Stanford University

<https://get-zero-paper.github.io>

**Abstract:** This paper introduces GET-Zero, a model architecture and training procedure for learning an embodiment-aware control policy that can immediately adapt to new hardware changes without retraining. To do so, we present Graph Embodiment Transformer (GET), a transformer model that leverages the embodiment graph connectivity as a learned structural bias in the attention mechanism. We use behavior cloning to distill demonstration data from embodiment-specific expert policies into an embodiment-aware GET model that conditions on the hardware configuration of the robot to make control decisions. We conduct a case study on a dexterous in-hand object rotation task using different configurations of a four-fingered robot hand with joints removed and with link length extensions. Using the GET model along with a self-modeling loss enables GET-Zero to zero-shot generalize to unseen variation in graph structure and link length, yielding a 20% improvement over baseline methods. All code and qualitative video results are on our [project website](#).

**Keywords:** Cross-embodiment learning, Dexterous manipulation

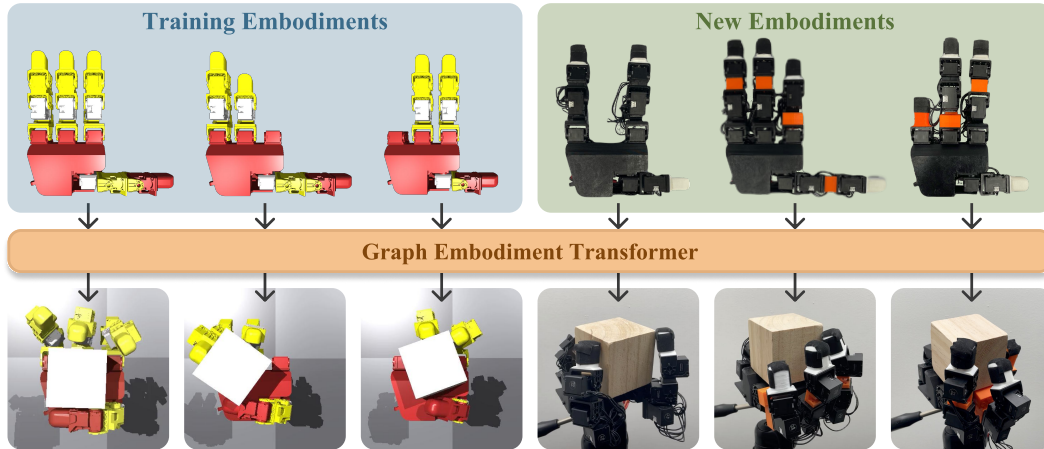


Figure 1: **GET-Zero** is an embodiment-aware policy that is able to zero-shot generalize to unseen embodiment designs with varied geometry, number of joints, and graph structure.

## 1 Introduction

Learning algorithms have significantly improved robots’ ability to sense and adapt to external environments, yet most robots today cannot tolerate minor changes in their internal hardware. From missing links caused by damage to added joints for design improvements, hardware modifications often require retraining existing policies with embodiment-specific data.

Recent methods develop embodiment-aware policies that condition on the hardware configuration of a robot design to control a class of embodiments [1, 2, 3, 4, 5, 6], which enables efficient data reuse across embodiments. However, these methods often have incomplete embodiment representations which ignore the graph connectivity of the robot, and thus cannot generalize well to an embodiment with a varied graph structure. Improving the performance under graph variations would greatly

expand the applicability of embodiment-aware methods in domains such as manipulation, where the number of fingers may vary or in locomotion, where the leg may have a varying number of joints.

Motivated by this limitation, the goal of this work is to introduce an embodiment representation that explicitly leverages the graph connectivity of the robot to improve zero-shot control of robots with variations in graph structure. We propose GET-Zero, which introduces the **Graph Embodiment Transformer (GET)** model architecture that enables **zero-shot adaptation** to new embodiments (Fig. 1). The key idea of GET is to leverage the robot graph connectivity as a structural bias in the transformer attention mechanism. By training this model using behavior data from a variety of robot embodiments, we can then zero-shot control previously unseen embodiments with varied geometry, number of joints, and graph structure. Specifically, GET-Zero consist of three novel components:

1. **Graph Embodiment Transformer (GET).** GET is a modified transformer architecture [7] that encodes joints as separate tokens and uses the embodiment connectivity as a learned bias in the transformer attention mechanism. Attention enables local joint information to communicate and the graph attention bias modulates this communication based on how the joints are physically connected. This extends prior embodiment-aware transformer models which either do not encode the embodiment connectivity [3] or have incomplete graph representations [4].
2. **Embodiment-Aware Distillation.** To train GET-Zero we first collect demonstration data from embodiment-specific experts. By conditioning on embodiment information, we then distill knowledge from embodiment-specific experts into an embodiment-aware GET model using behavior cloning (BC) that controls both training and unseen embodiments with a *single* set of network weights. Our approach contrasts with prior methods [2, 3, 4] that use RL to simultaneously learn an embodiment-aware model while learning to complete the task across all embodiments, which is significantly more difficult and prevents the use of expert demonstration data.
3. **Self Modeling Loss.** During the distillation BC phase, we introduce an additional self modeling loss alongside the standard policy action loss. The self-modeling output predicts the position of each joint in 3D space (i.e., forward kinematics), which encourages the network to understanding the embodiment graph and infer actions accordingly. We found that this simple and general supervision improves generalization performance.

To validate GET-Zero, we conduct a case study to learn an embodiment-aware, dexterous in-hand object rotation policy across different hardware configurations of a multi-fingered robot hand. In particular, we use the LEAP Hand [8], which is a low-cost, four-fingered hand with four joints per finger consisting of 3D printed components and off-the-shelf motors. We create 44 hardware configurations of this hand by removing different combinations of finger joints and associated links. Next, we train embodiment-specific expert policies for each hand using RL in simulation and then follow the GET-Zero training procedure to distill the expert behavior into an embodiment-aware GET model. Our experiments in simulation and real world demonstrate how the novel graph encoding and self-modeling in GET-Zero improves the capability of this model to zero-shot control hand designs with unseen variations in link geometry and graph connectivity.

## 2 Related Work

**Cross-Embodiment pretraining with embodiment-specific finetuning.** Recent approaches leverage large-scale pretraining, either on visual data, robot trajectories, language, or tasks as an initialization for policy learning or generalist agents [9, 10, 11, 12, 13, 14, 15]. Other approaches leverage robot data across embodiments to initialize a generalist agent, and then fine-tune the base model or an action head to adapt to a new robot embodiments [16, 17]. These method often assume a unified action space, which is reasonable for navigation [18] or for robot arm policies where the end-effector pose is a shared representation across arms [17, 19, 16, 20]. However, unified actions spaces are often not sufficient for tasks where precise, low-level joint actions matter, such as dexterous manipulation [21, 22, 23, 24]. Moreover, many approaches still require non-trivial amounts of additional training data specific to the target hardware and environment. Instead, our method uses the graph structure of the robot as a general embodiment representation to improve zero-shot transfer for tasks where a unified action space is not possible.

**Embodiment Representation.** Prior works in multi-embodiment policies demonstrate using a single policy to control different robot designs [1, 25, 2, 3, 4, 6, 5]. However, most methods show limited generalization ability to new embodiment designs beyond the training set due to incomplete embodiment representations. For example, Octo [1] has 3rd-person images of the robot arm which doesn’t generalize across robot appearance changes, though this could be addressed with robot inpainting [26]. Other methods learn cross embodiments representations that align actions across different embodiments [27, 28, 29]. In contrast, GET-Zero uses the graph embodiment structure connecting local sensory information as a flexible and general representation across robots.

**Embodiment-aware policy architectures.** Most related to our approach is the line of work developing embodiment-aware policies. Prior methods [30, 31, 2] structure a graph neural network (GNN) to match the embodiment graph with joints as nodes and links as edges to control stick-like walking characters in simulation. Kurin et al. [3] shows that a GNN matching the embodiment graph is outperformed with the fully connected attention mechanism in transformers [7] despite having no graph encoding. Gupta et al. [4] extends this model with dynamics and kinematics encodings, demonstrating zero-shot generalization to these properties. However, these methods do not generalize well to unseen embodiment graphs due to no [3] or limited [4] graph representations. Our method GET-Zero extends the transformer architecture in [3, 4] to include an explicit graph representation that improves zero-shot generalization to unseen embodiment graphs. Furthermore, unlike prior embodiment-aware RL methods that do locomotion only in simulation [30, 31, 2, 3, 4], GET-Zero uses behavior cloning from experts for an in-hand rotation task transferable to a real robot.

### 3 Method: Graph Embodiment Transformer

We present Graph Embodiment Transformer (GET), an embodiment-aware transformer encoder [7] that uses the embodiment graph as a structural bias in network architecture (Fig. 2). An embodiment graph consists of nodes representing local joint information and directed edges representing links connecting parent and child joints. GET represents each joint as separate transformer tokens containing both local sensory observations and local hardware properties (§3.1). The graph edges (i.e., links) are encoded through a learned attention bias in the self-attention layers (§3.2).

#### 3.1 Embodiment Tokenization

For a robot with  $J$  joints, there are  $J$  input tokens to the transformer encoder containing local observations and  $J$  corresponding output tokens for per-joint actions. The encoder supports a variable number of tokens which enables compatibility as the number of joints varies across embodiments.

Observations can either be local  $l$  to specific joints or global  $g$  across the entire embodiment. Additionally, observations are either fixed  $f$  or variable  $v$  if they change during execution. This yields four observation types: variable local  $o_{vl}$  (e.g., joint angle/velocity), variable global  $o_{vg}$  (e.g., a global time encoding, or environment state), fixed local  $o_{fl}$  (e.g., joint position in rest pose, or joint limit ranges) and fixed global  $o_{fg}$  (e.g., a task identifier).  $H$  past history steps are included only for variable observations ( $o_{vl}$  and  $o_{vg}$ ). The local observations for joint  $j$  are defined as  $o_{*,l,j}$ . The transformer token  $T_j$  for joint  $j$  at timestep  $t$  is constructed as  $T_j^t = [o_{vg}^{t \rightarrow t-H}, o_{fg}, o_{vl,j}^{t \rightarrow t-H}, o_{fl,j}]$ . The tokens pass through a learned linear embedding before entering the transformer encoder.

#### 3.2 Graph Encoding

One challenge is that the transformer encoder has no direct graph encoding mechanism in the original implementation [7]. Input tokens are permutation invariant without a positional encoding mechanism, but are often linearly encoded with sinusoidal or learned positional encodings. Prior embodiment-aware methods address this in multiple ways. Kurin et al. [3] use no positional encoding meaning no graph representation is present. Gupta et al. [4] linearize the graph using a depth-first search ordering then apply a learned linear positional encoding. However, this approach is sensitive to graph variations as the DFS ordering is not unique, which empirically caused a  $\sim 75\%$  drop in performance with the opposite node order in Gupta et al. [4]. Sferrazza et al. [32] use the adjacency matrix as a binary attention mask to limit communication early in the transformer to adjacent nodes.

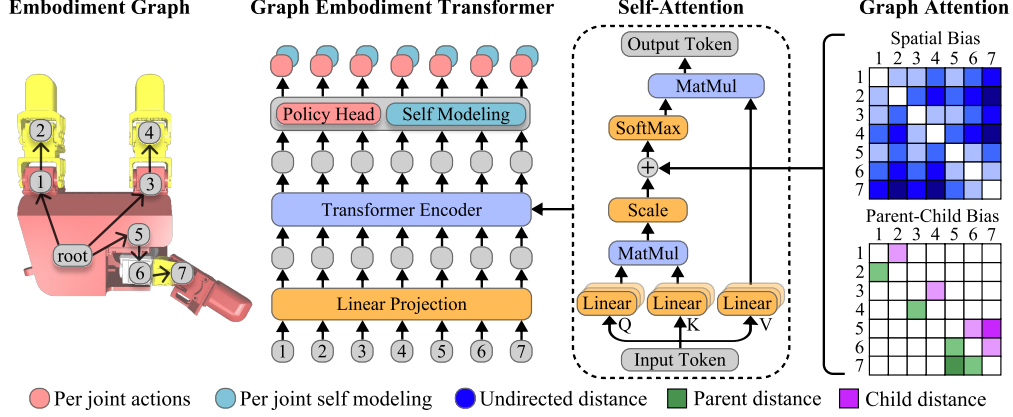


Figure 2: **Graph Embodiment Transformer (GET)**. GET is an embodiment-aware model based on a transformer encoder. Each joint forms separate tokens containing local sensory and embodiment information. The self-attention layers use an undirected (Spatial Bias) and directed (Parent-Child Bias) graph distance to bias the attention scores between joints according to the embodiment graph (grid color intensity indicates distance between nodes). A policy head predicts actions and a self modeling head predicts meta-properties about the embodiment, such as forward kinematics.

Our GET model uses a learned attention bias in the encoder self-attention mechanism to explicitly encode the graph similar to the Graphormer work by Ying et al. [33]. Using the notation from Ying et al. [33], the inputs to the self-attention layer given  $J$  joints are the hidden states  $H = [h_1^\top, \dots, h_J^\top] \in \mathbb{R}^{J \times d}$ .  $H$  is projected by three matrices  $W_Q \in \mathbb{R}^{d \times d_K}$ ,  $W_K \in \mathbb{R}^{d \times d_K}$ ,  $W_V \in \mathbb{R}^{d \times d_V}$  to produce  $Q = HW_Q$ ,  $K = HW_K$ ,  $V = HW_V$ . Then the attention layers will compute an attention matrix  $A \in \mathbb{R}^{J \times J}$  where  $A_{ij}$  represents the attention score computed between joints  $i$  and  $j$  as follows:  $A = QK^\top / \sqrt{d}$ ,  $\text{Attn}(H) = \text{softmax}(A)V$ .

To encode the embodiment graph, we learn two separate biases to the attention scores ( $A$ ): a Spatial Encoding [33], and a novel Parent-Child Encoding, detailed below.

**Spatial Encoding.** The spatial encoding computes the shortest path distance (SPD)  $\phi^{\text{SPD}}$  between node  $i$  and node  $j$  in the graph as  $\phi^{\text{SPD}}(i, j)$ . An embedding table  $s$  is indexed with the SPD distance as  $s_{\phi^{\text{SPD}}(i, j)}$  to produce a learned scalar that is added on top of the attention score  $A_{ij}$ .

The intuition is that the attention mechanism can learn to pay more or less attention to joints in the graph based on their distance. For example, nearby joints may learn a large attention bias, while far away joints that may not have much influence on each other hence a low spatial bias.

**Parent-Child Encoding.** Unlike Graphormer [33] that only encodes undirected graph in the attention mechanism, we introduce a new parent-child attention bias to encode directed features. For joints  $i$  and  $j$ , we compute the parent distance  $\phi^P(i, j) = \phi^{\text{SPD}}(i, j) \mathbb{1}\{i \text{ is parent of } j\}$  which is the distance between  $i$  and  $j$  if  $j$  is the child of  $i$  at some distance along the forward kinematic chain, otherwise 0. We compute an analogous formula for the child distance as  $\phi^C(i, j) = \phi^{\text{SPD}}(i, j) \mathbb{1}\{i \text{ is child of } j\}$ . There are associated scalar embedding tables  $p$  and  $c$ .

The intuition is that the model may attempt to compute forward kinematics through the embodiment graph and the parent-child encoding enables the model to modulate attention based on directed nature of a forward chain (child joint angles do not impact the parent joint’s 3D pose).

**Attention Bias Computation.** For each attention head and encoder layer, we have separate embeddings  $s$ ,  $p$ , and  $c$  and compute attention as:  $A_{ij} = \frac{(h_i W_Q)(h_j W_K)^T}{\sqrt{d}} + s_{\phi^{\text{SPD}}(i, j)} + p_{\phi^P(i, j)} + c_{\phi^C(i, j)}$ . One key aspect of this approach is that this attention bias is invariant to the ordering of the input tokens unlike the depth-first linearization approach [4].

**Output Heads.** After passing  $J$  tokens through each transformer encoder, GET produces  $J$  corresponding latent features. We include a policy head to predict actions and a self-modeling head used to predict meta-features about the embodiment. Further details on these heads are discussed in §4.3.

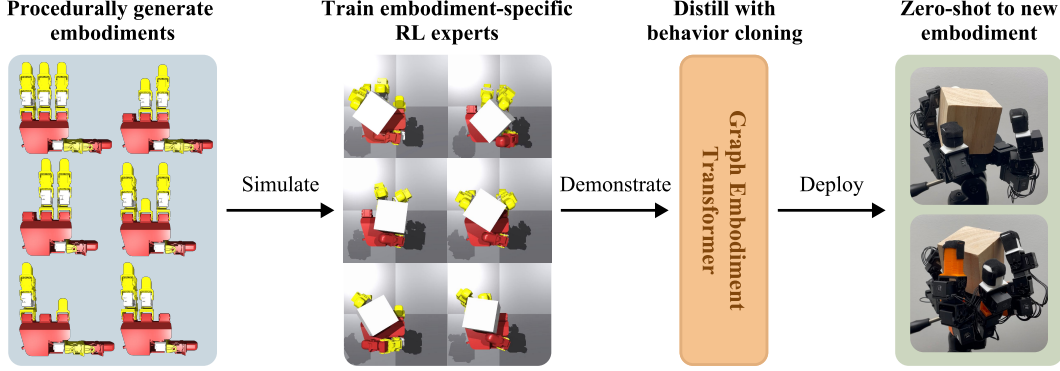


Figure 3: **Training procedure.** To train GET-Zero, we follow a teacher-student paradigm, where the teachers are *separate* embodiment-specific experts trained using RL. Then we distill knowledge from the experts into a *single* embodiment-aware transformer (i.e., the student policy) using behavior cloning with a self-modeling loss. GET-Zero takes as input embodiment definition and proprioception, and infers proper actions to perform an in-hand rotation task for an unseen embodiment.

## 4 Case Study: In-hand Object Rotation

We conduct a case study on applying GET-Zero to an in-hand object rotation task with different variations of LEAP Hand [8]. Unlike pick-and-place tasks where a unified action space across different robot arms is easy to define (e.g., end-effector space), the task of in-hand object rotation requires the policy to differentiate low-level joint space actions that are aware of the embodiment structure. Applying GET-Zero to the in-hand rotation task requires three stages (Fig. 3): 1) generate embodiment variations (§4.1), 2) train embodiment-specific experts using RL (§4.2), and 3) distill knowledge from experts into an embodiment-aware GET architecture (§4.3).

### 4.1 Procedural Embodiment Generation

The LEAP Hand [8] consists of 3D printed components and off-the-shelf motors, making it highly configurable. The hand features three main fingers which are identical in structure and a thumb which has a separate structure. For the main fingers, we construct five variations of the fingers (4 combinations + no finger config) and two different variations of the thumb by removing various combinations of joints (Fig. 4). This yields  $5^3 \times 2 = 250$  embodiment configurations from which we require 1) at least two fingers have at least one joint and 2) that there is at least one main finger with two joints, yielding 236 graph variation embodiments. We additionally introduce 1.5cm link length extensions shown in orange in Fig. 4 to the 236 designs to generate additional hand designs.

### 4.2 Train Embodiment-Specific Experts

We train embodiment-specific RL experts using PPO [34] in Isaac Gym [35] to complete the in-hand rotation task, adapted from the setup by Shaw et al. [8]. This setup consists of rewards for rotation along the yaw axis, penalties for high motor torques and dropping the cube, and domain randomization across cube sizes. These learned policies operate only on proprioceptive joint states and predict delta joint targets that guide a PD controller. We pick the best of five training seeds for each embodiment and filter out embodiments that are not able to complete a full  $2\pi$  rotation within 30s. Many hand designs are unable to complete the rotation task under this threshold due to many missing joints, resulting in 44 training embodiments with associated expert policies.

### 4.3 Distill Experts into Embodiment-Aware Transformer

By rolling out embodiment-specific experts we can collect demonstration data for each hand. Specifically, we collect 7 hours worth of demonstrations for each embodiment. This demonstration data is combined with embodiment information to form the training dataset of (state, action, embodiment) tuples used to train the embodiment-aware GET model with behavior cloning (BC).

Separating the collection of demonstration data from the training of embodiment-aware policies gives more freedom to use any existing policy architecture or training setup to generate expert



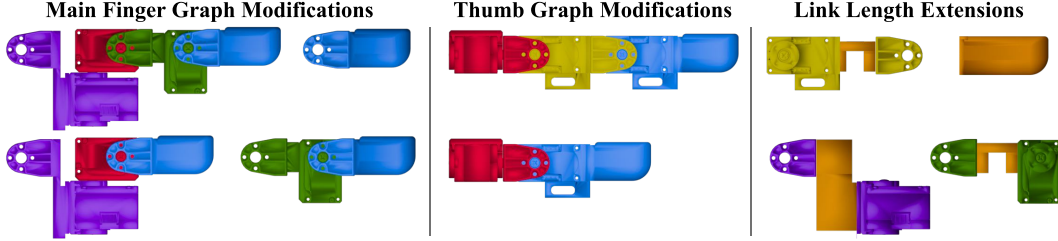


Figure 4: **Finger Variations.** We procedurally generate variations of the fingers in the LEAP Hand [8] by removing joints and links as well as adding in 1.5cm link length extensions (orange).

demonstrations (e.g. teleoperation, RL, optimization based methods, privileged information, etc.). Prior embodiment-aware methods [3, 4] do not separate these stages and instead jointly learn the embodiment-aware policy along with learning how to control training embodiments.

**GET Training Setup.** We train the GET architecture (§3) using BC. Specifically, our token input consists normalized joint angles and PD target joint states ( $o_{vl}$ ), 3D joint position and joint rotation with respect to the parent joint from the URDF file ( $o_{fl}$ ), and a sinusoidal phase encoding with a period of two seconds to encode cyclic progression through the rotation cycle ( $o_{vg}$ ). The directed embodiment graph is an additional input used in the graph attention encoding (§3.2).

**Policy Head.** The network contains a policy head for predicting single-step action. Each joint has a PD target state that is initialized to the starting joint state. The action head predicts delta actions that are added to this target state, which sets the target state for the low-level PD controller. We supervise these actions using  $L_2$  loss with the demonstration data.

**Self-Model Head.** The network also has a self-modeling head to predict the current 3D pose of each joint in the robot local frame. This forward kinematics (FK) task is simple and generally applicable across embodiments, yet requires the network to use the spatial relationships from the graph and current joint angles along the FK chain. We supervise with the ground truth FK pose with  $L_2$  loss. As the policy and self-modeling heads operate on the same latent representations output by GET, self-modeling encourages the actions to be predictable from an embodiment-rich representation.

## 5 Experiments

We procedurally generate 236 graph variations of the LEAP hand [8] by removing various combinations of joints and associated links from the embodiment (§4.1). From these, we obtain 44 embodiments with graph variations with associated expert RL policies that achieve a baseline level of performance (§4.2). These 44 embodiments serve as training embodiments and only have graph variations (link length extensions are not seen during training). Our experiments consist of using demonstration data from these embodiments to train various baselines and ablations of the GET architecture to evaluate zero-shot performance to unseen embodiment graphs and link extensions.

**Comparisons.** MetaMorph [4] and Amorpheus [3] models are two prior embodiment-aware transformer methods. These methods also use a transformer but do not contain a full graph encoding or self modeling loss. We re-implement the positional encoding aspects of these method in our setup to focus on comparing the impact of our graph representation and self-modeling rather than differences in task (locomotion v.s. manipulation), training procedure (RL v.s. BC) or observation format.

- **ET.** The Embodiment Transformer (ET) matches the architecture and token format of GET except without the graph encoding (§3.2) or the self modeling loss. This ET baseline most similarly matches the encoding method in Amorpheus [3], which uses no graph encoding. This means that the model has no explicit connectivity information about the joints.
- **ET+DFS.** This baseline uses the same positional encoding scheme as MetaMorph [4] that linearizes the embodiment graph in depth-first search (DFS) ordering and then applies a learned positional encoding onto the linear sequence.

We also ablate different components of our method such as self-modeling loss (SL), spatial encoding (SE), parent-child encoding (PE). Results are summarized in Tab. 1.

	Training Graph	New Graph	New Geo	New Graph & Geo
RL experts	16.50	—	—	—
ET [3]	14.82±0.15	8.68±0.34	12.92±0.36	8.12±0.46
ET+DFS [4]	15.03±0.37	6.45±0.28	14.37±0.34	6.27±0.22
ET+SL	14.68±0.33	8.19±0.74	12.71±0.72	7.60±1.12
ET+PE+SE	16.03±0.19	9.65±0.23	15.30±0.29	9.05±0.42
ET+PE+SL	16.10±0.22	9.56±0.47	15.59±0.32	8.81±0.42
ET+SE+SL	16.24±0.21	10.04±0.15	15.74±0.25	<b>9.75±0.20</b>
ET+PE+SE+SL (GET-Zero)	<b>16.32±0.24</b>	<b>10.07±0.58</b>	<b>15.80±0.29</b>	<b>9.75±0.54</b>

Table 1: **Simulation results (average rotational velocity deg/sec).** RL experts are embodiment-specific policies. ET: Embodiment transformer, DFS: depth-first graph encoding, SL: self-modeling loss, SE: spatial graph encoding, PE: parent-child graph encoding. We observe GET-Zero consistently outperforms prior works [3, 4] through the use of graph encoding and self-modeling meta-task.

**Evaluation Metric.** The task performance is measured by average rotational velocity along the yaw axis in degrees/second including standard deviation across five seeds. We compute results by rolling out the embodiment-aware policies in a physics simulator for a total of 42 minutes of execution time per embodiment per seed. Each category averages over 10 unseen embodiments (Appendix Fig. 6).

### 5.1 Key Results and Findings

Table 1 summarizes GET-Zero’s performance on training embodiments (Training Graph) and on multiple categories of zero-shot embodiments: unseen graph variations (New Graph), unseen link length variations (New Geo) and both (New Graph & Geo). Note that link length variations (Fig. 4) were never seen during training.

**GET-Zero matches the performance of embodiment-specific experts on training embodiments.** Despite being trained to control 44 embodiments with graph changes, GET-Zero reaches 99% of the performance of the embodiment-specific RL experts with a *single* set of network weights (Tab. 1).

**GET-Zero improves zero-shot capabilities to graph and geometry variations.** Compared to the best performing baseline for each category, GET-Zero achieves a 16% improvement with zero-shot to new graph, an 10% improvement with zero-shot to link length variations, and a 20% improvement with zero-shot to both graph and link length variations (Tab. 1).

**Self-modeling improves performance only with graph encoding present.** We observe that adding self-modeling (SL) to the baseline (ET) consistently decreases zero-shot performance by an average of 4.6% across the three categories, but yields an average increase of 5.1% when added to the model with graph encoding (ET+PE+SE) (Table 1). This result intuitively makes sense as the ET baseline has no graph encoding which is needed to complete the forward kinematics task and thus self-modeling provides a poor training signal. In the presence of graph encoding, forward kinematics serves as a useful meta-task to improve cross-embodiment transfer.

**Depth-first graph linearization lowers performance under graph variations.** The DFS linearization (ET+DFS) serves as a simple, yet incomplete graph representation as the DFS ordering is not unique. Additionally, if a joint earlier in the linearization is removed, then all subsequent joints will shift down and receive a new positional encoding. When only link length variations are present, linearization improves zero-shot performance over no positional encoding (ET) by 11% (Tab. 1). However, when unseen graph changes are present, performance drops by 26%. This result intuitively makes sense as the linearized positional encoding can overfit to training embodiment graphs, but fails to generalize with graph changes due to the aforementioned issue with DFS. This motivates the need for the more complete graph representation used in GET-Zero.

**Spatial and parent-child encoding help policy learning.** Relative to ET with self-modeling (ET+SL), adding the parent-child graph encoding (ET+PE+SL) improves performance by 19% and adding the spatial graph encoding (ET+SE+SL) improves performance by 25% on average across zero-shot tasks. We note that adding parent-child encoding provides only a minor improvement when the spatial encoding is present, but that best performance is when both encodings are present.








						
Variation	Training	New Graph	New Graph	New Geo	New Graph+Geo	New Graph+Geo
ET	11.5, 55%, 0	5.9, 50%, 0	9.2, 93%, 1	8.6, 57%, 2	9.6, 67%, 18	-0.6, -6%, 0
GET-Zero	20.5, 70%, 0	8.3, 65%, 0	21.8, 133%, 0	19.0, 83%, 1	9.0, 53%, 16	1.2, 9%, 0

Table 2: **Real world evaluation.** We evaluate sim-to-real capabilities of GET-Zero and the ET baseline on LEAP Hand [8] design variations. [Col 1] An AR tag tracks cube rotation. [Col 2] The unmodified LEAP Hand (seen during training). [Col 3-7] Zero-shot embodiments with unseen graph variations and/or link length extensions (orange). We report (across 3 minute trial): 1) average cube angular velocity in degrees/second 2) real average velocity as a % of sim average velocity for the same embodiment and policy (sim-to-real gap) and 3) number of times the hand dropped the cube.

**Training diversity improves zero-shot.** As shown in Fig. 5, increasing diversity of training embodiments improves zero shot generalization performance to unseen graph changes. GET-Zero also achieve a reasonable rotation performance even with only 10 training embodiments, and we observe that GET-Zero achieves more data efficient generalization performance than ET.

## 5.2 Real-world Evaluation

We present results from a real-world evaluation of GET-Zero on unseen embodiments in Tab. 2. We observe GET-Zero outperforms the ET baseline for both the original LEAP Hand [8] as well as unseen graph and link length variations. Empirically, the baseline ET policy struggles to continuously rotate the cube, and we observe high finger precision is required for stable control. We observe a sim-to-real gap, but GET-Zero achieves zero-shot performance above simulation for the third embodiment. For another embodiment (second from right), a missing index finger causes the hand to drop the cube many times. For the right-most embodiment, a shortened index finger and thumb make it challenging for the hand to start the rotation cycle. Training with link length extensions could help improve zero-shot performance to New Graph+Geo. Please refer to the appendix for real-world evaluation methodology and the website for videos.

## 5.3 Limitations

While GET-Zero improves zero-shot performance, it’s unlikely that our model trained on LEAP Hand configurations would zero-shot transfer to a different robot hand. For example, we train with at most 16 joints, and expect poor performance for hands with more joints or fingers. Through compatible with the GET tokenization, our model does not explicitly encode joint limit ranges, motor strength, friction properties or finger shape, all of which vary with a new hand and are important in manipulation tasks. We also assume that the hand design space has enough variations to train on to expect reasonable generalization performance. Additionally, GET-Zero assumes a fixed set of embodiments, though future work could extend the model to iteratively improve a robot’s design.

## 6 Conclusion

We present GET-Zero, an embodiment-aware model architecture and training procedure that enables zero-shot control of new robot designs. Through a case study on an in-hand object rotation task, we demonstrate the ability of our model to control a wide range of hardware configurations of a multi-fingered robot hand under variations in embodiment graph and geometry. Our results in simulation and real demonstrate that the graph encoding and self-modeling features in GET-Zero improve cross-embodiment transfer. Our goal is for GET-Zero to serve as a useful, embodiment-aware method for the robotics community to share knowledge across similar robot designs.

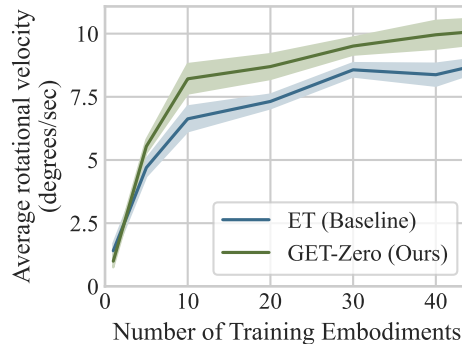


Figure 5: **Impact of training embodiments on zero-shot graph generalization.**



## Acknowledgments

We would like to thank Kenneth Shaw, Prof. Pathak’s lab at CMU, and the Prof. Liu’s Movement lab at Stanford for sharing the LEAP Hand hardware. We would also like to thank Huy Ha, Xiaomeng Xu, Mengda Xu and Haochen Shi for their helpful feedback and fruitful discussions. This work was supported in part by Sloan Fellowship and NSF #2132519. The views and conclusions contained herein are those of the authors and should not be interpreted as necessarily representing the official policies, either expressed or implied, of the sponsors.

## References

- [1] Octo Model Team, D. Ghosh, H. Walke, K. Pertsch, K. Black, O. Mees, S. Dasari, J. Hejna, C. Xu, J. Luo, T. Kreiman, Y. Tan, D. Sadigh, C. Finn, and S. Levine. Octo: An open-source generalist robot policy. <https://octo-models.github.io>, 2023.
- [2] W. Huang, I. Mordatch, and D. Pathak. One policy to control them all: Shared modular policies for agent-agnostic control. In *ICML*, 2020.
- [3] V. Kurin, M. Igl, T. Rocktäschel, W. Boehmer, and S. Whiteson. My body is a cage: the role of morphology in graph-based incompatible control. In *International Conference on Learning Representations*, 2021. URL <https://openreview.net/forum?id=N3zUDGN510>.
- [4] A. Gupta, L. Fan, S. Ganguli, and L. Fei-Fei. Metamorph: Learning universal controllers with transformers. In *International Conference on Learning Representations*, 2022. URL [https://openreview.net/forum?id=0pmqtk\\_GvYL](https://openreview.net/forum?id=0pmqtk_GvYL).
- [5] M. Shafiee, G. Bellegarda, and A. Ijspeert. Manyquadrupeds: Learning a single locomotion policy for diverse quadruped robots. *arXiv preprint arXiv:2310.10486*, 2023.
- [6] N. Bohlinger, G. Czechmanowski, M. P. Krupka, P. Kicki, K. Walas, J. Peters, and D. Tateo. One policy to run them all: Towards an end-to-end learning approach to multi-embodiment locomotion. In *Workshop on Embodiment-Aware Robot Learning*, 2024. URL <https://openreview.net/forum?id=HVWusz2zv5>.
- [7] A. Vaswani, N. Shazeer, N. Parmar, J. Uszkoreit, L. Jones, A. N. Gomez, L. u. Kaiser, and I. Polosukhin. Attention is all you need. In I. Guyon, U. V. Luxburg, S. Bengio, H. Wallach, R. Fergus, S. Vishwanathan, and R. Garnett, editors, *Advances in Neural Information Processing Systems*, volume 30. Curran Associates, Inc., 2017. URL [https://proceedings.neurips.cc/paper\\_files/paper/2017/file/3f5ee243547dee91fbd053c1c4a845aa-Paper.pdf](https://proceedings.neurips.cc/paper_files/paper/2017/file/3f5ee243547dee91fbd053c1c4a845aa-Paper.pdf).
- [8] K. Shaw, A. Agarwal, and D. Pathak. Leap hand: Low-cost, efficient, and anthropomorphic hand for robot learning. *Robotics: Science and Systems (RSS)*, 2023.
- [9] A. Brohan, N. Brown, J. Carbajal, Y. Chebotar, X. Chen, K. Choromanski, T. Ding, D. Driess, A. Dubey, C. Finn, P. Florence, C. Fu, M. G. Arenas, K. Gopalakrishnan, K. Han, K. Hausman, A. Herzog, J. Hsu, B. Ichter, A. Irpan, N. Joshi, R. Julian, D. Kalashnikov, Y. Kuang, I. Leal, L. Lee, T.-W. E. Lee, S. Levine, Y. Lu, H. Michalewski, I. Mordatch, K. Pertsch, K. Rao, K. Reymann, M. Ryoo, G. Salazar, P. Sanketi, P. Sermanet, J. Singh, A. Singh, R. Soricut, H. Tran, V. Vanhoucke, Q. Vuong, A. Wahid, S. Welker, P. Wohlhart, J. Wu, F. Xia, T. Xiao, P. Xu, S. Xu, T. Yu, and B. Zitkovich. Rt-2: Vision-language-action models transfer web knowledge to robotic control. In *arXiv preprint arXiv:2307.15818*, 2023.
- [10] I. Radosavovic, B. Shi, L. Fu, K. Goldberg, T. Darrell, and J. Malik. Robot learning with sensorimotor pre-training. In *Conference on Robot Learning*, pages 683–693. PMLR, 2023.
- [11] S. Reed, K. Zolna, E. Parisotto, S. G. Colmenarejo, A. Novikov, G. Barth-maroon, M. Giménez, Y. Sulsky, J. Kay, J. T. Springenberg, T. Eccles, J. Bruce, A. Razavi, A. Edwards, N. Heess,

- Y. Chen, R. Hadsell, O. Vinyals, M. Bordbar, and N. de Freitas. A generalist agent. *Transactions on Machine Learning Research*, 2022. ISSN 2835-8856. URL <https://openreview.net/forum?id=1ikK0kHjvj>. Featured Certification, Outstanding Certification.
- [12] I. Schubert, J. Zhang, J. Bruce, S. Bechtle, E. Parisotto, M. Riedmiller, J. T. Springenberg, A. Byravan, L. Hasenclever, and N. Heess. A generalist dynamics model for control. *arXiv preprint arXiv:2305.10912*, 2023.
- [13] A. Stone, T. Xiao, Y. Lu, K. Gopalakrishnan, K.-H. Lee, Q. Vuong, P. Wohlhart, S. Kirmani, B. Zitkovich, F. Xia, C. Finn, and K. Hausman. Open-world object manipulation using pre-trained vision-language models. In *arXiv preprint*, 2023.
- [14] D. Driess, F. Xia, M. S. M. Sajjadi, C. Lynch, A. Chowdhery, B. Ichter, A. Wahid, J. Tompson, Q. Vuong, T. Yu, W. Huang, Y. Chebotar, P. Sermanet, D. Duckworth, S. Levine, V. Vanhoucke, K. Hausman, M. Toussaint, K. Greff, A. Zeng, I. Mordatch, and P. Florence. Palm-e: An embodied multimodal language model. In *arXiv preprint arXiv:2303.03378*, 2023.
- [15] D. Kalashnikov, A. Irpan, P. Pastor, J. Ibarz, A. Herzog, E. Jang, D. Quillen, E. Holly, M. Kalakrishnan, V. Vanhoucke, et al. Scalable deep reinforcement learning for vision-based robotic manipulation. In *Conference on robot learning*, pages 651–673. PMLR, 2018.
- [16] O. X.-E. Collaboration, A. Padalkar, A. Pooley, A. Jain, A. Bewley, A. Herzog, A. Irpan, A. Khazatsky, A. Rai, A. Singh, A. Brohan, A. Raffin, A. Wahid, B. Burgess-Limerick, B. Kim, B. Schölkopf, B. Ichter, C. Lu, C. Xu, C. Finn, C. Xu, C. Chi, C. Huang, C. Chan, C. Pan, C. Fu, C. Devin, D. Driess, D. Pathak, D. Shah, D. Büchler, D. Kalashnikov, D. Sadigh, E. Johns, F. Ceola, F. Xia, F. Stulp, G. Zhou, G. S. Sukhatme, G. Salhotra, G. Yan, G. Schiavi, H. Su, H.-S. Fang, H. Shi, H. B. Amor, H. I. Christensen, H. Furuta, H. Walke, H. Fang, I. Mordatch, I. Radosavovic, I. Leal, J. Liang, J. Kim, J. Schneider, J. Hsu, J. Bohg, J. Bingham, J. Wu, J. Wu, J. Luo, J. Gu, J. Tan, J. Oh, J. Malik, J. Tompson, J. Yang, J. J. Lim, J. Silvério, J. Han, K. Rao, K. Pertsch, K. Hausman, K. Go, K. Gopalakrishnan, K. Goldberg, K. Byrne, K. Oslund, K. Kawaharazuka, K. Zhang, K. Majd, K. Rana, K. Srinivasan, L. Y. Chen, L. Pinto, L. Tan, L. Ott, L. Lee, M. Tomizuka, M. Du, M. Ahn, M. Zhang, M. Ding, M. K. Srirama, M. Sharma, M. J. Kim, N. Kanazawa, N. Hansen, N. Heess, N. J. Joshi, N. Suenderhauf, N. D. Palo, N. M. M. Shafiullah, O. Mees, O. Kroemer, P. R. Sanketi, P. Wohlhart, P. Xu, P. Sermanet, P. Sundaresan, Q. Vuong, R. Rafailov, R. Tian, R. Doshi, R. Martín-Martín, R. Mendonca, R. Shah, R. Hoque, R. Julian, S. Bustamante, S. Kirmani, S. Levine, S. Moore, S. Bahl, S. Dass, S. Song, S. Xu, S. Haldar, S. Adebola, S. Guist, S. Nasiriany, S. Schaal, S. Welker, S. Tian, S. Dasari, S. Belkhale, T. Osa, T. Harada, T. Matsushima, T. Xiao, T. Yu, T. Ding, T. Davchev, T. Z. Zhao, T. Armstrong, T. Darrell, V. Jain, V. Vanhoucke, W. Zhan, W. Zhou, W. Burgard, X. Chen, X. Wang, X. Zhu, X. Li, Y. Lu, Y. Chebotar, Y. Zhou, Y. Zhu, Y. Xu, Y. Wang, Y. Bisk, Y. Cho, Y. Lee, Y. Cui, Y. hua Wu, Y. Tang, Y. Zhu, Y. Li, Y. Iwasawa, Y. Matsuo, Z. Xu, and Z. J. Cui. Open X-Embodiment: Robotic learning datasets and RT-X models. <https://arxiv.org/abs/2310.08864>, 2023.
- [17] K. Bousmalis, G. Vezzani, D. Rao, C. Devin, A. X. Lee, M. Bauza, T. Davchev, Y. Zhou, A. Gupta, A. Raju, et al. Robocat: A self-improving foundation agent for robotic manipulation. *arXiv preprint arXiv:2306.11706*, 2023.
- [18] D. Shah, A. Sridhar, N. Dashora, K. Stachowicz, K. Black, N. Hirose, and S. Levine. Vint: A foundation model for visual navigation. *arXiv preprint arXiv:2306.14846*, 2023.
- [19] J. Yang, C. Glossop, A. Bhorkar, D. Shah, Q. Vuong, C. Finn, D. Sadigh, and S. Levine. Pushing the limits of cross-embodiment learning for manipulation and navigation. *arXiv preprint arXiv:2402.19432*, 2024.
- [20] R. Martín-Martín, M. Lee, R. Gardner, S. Savarese, J. Bohg, and A. Garg. Variable impedance control in end-effector space. an action space for reinforcement learning in contact rich tasks. In *Proceedings of the International Conference of Intelligent Robots and Systems (IROS)*, 2019.

- [21] L. Han and J. Trinkle. Dexterous manipulation by rolling and finger gaiting. In *Proceedings. 1998 IEEE International Conference on Robotics and Automation (Cat. No.98CH36146)*, volume 1, pages 730–735 vol.1, 1998. doi:10.1109/ROBOT.1998.677060.
- [22] J.-P. Saut, A. Sahbani, S. El-Khoury, and V. Perdereau. Dexterous manipulation planning using probabilistic roadmaps in continuous grasp subspaces. In *2007 IEEE/RSJ International Conference on Intelligent Robots and Systems*, pages 2907–2912, 2007. doi:10.1109/IROS.2007.4399090.
- [23] D. Rus. In-hand dexterous manipulation of piecewise-smooth 3-d objects. *The International Journal of Robotics Research*, 18(4):355–381, 1999. doi:10.1177/02783649922066268. URL <https://doi.org/10.1177/02783649922066268>.
- [24] Y. Bai and C. K. Liu. Dexterous manipulation using both palm and fingers. In *2014 IEEE International Conference on Robotics and Automation (ICRA)*, pages 1560–1565, 2014. doi:10.1109/ICRA.2014.6907059.
- [25] L. Shao, F. Ferreira, M. Jorda, V. Nambiar, J. Luo, E. Solowjow, J. A. Ojea, O. Khatib, and J. Bohg. Unigrasp: Learning a unified model to grasp with multifingered robotic hands. *IEEE Robotics and Automation Letters*, 5(2):2286–2293, 2020. doi:10.1109/LRA.2020.2969946.
- [26] L. Y. Chen, K. Hari, K. Dharmarajan, C. Xu, Q. Vuong, and K. Goldberg. Mirage: Cross-embodiment zero-shot policy transfer with cross-painting. In *Proceedings of Robotics: Science and Systems*, Delft, Netherlands, 2024.
- [27] M. Xu, Z. Xu, C. Chi, M. Veloso, and S. Song. XSkill: Cross embodiment skill discovery. In *7th Annual Conference on Robot Learning*, 2023. URL <https://openreview.net/forum?id=8L6pHd9aS6w>.
- [28] T. Chen, A. Murali, and A. Gupta. Hardware conditioned policies for multi-robot transfer learning. In *Advances in Neural Information Processing Systems*, pages 9355–9366, 2018.
- [29] K. Zakka, A. Zeng, P. Florence, J. Tompson, J. Bohg, and D. Dwibedi. Xirl: Cross-embodiment inverse reinforcement learning. *Conference on Robot Learning (CoRL)*, 2021.
- [30] T. Wang, R. Liao, J. Ba, and S. Fidler. Nervenet: Learning structured policy with graph neural networks. In *International Conference on Learning Representations*, 2018. URL <https://openreview.net/forum?id=S1sqHMZCb>.
- [31] D. Pathak, C. Lu, T. Darrell, P. Isola, and A. A. Efros. Learning to control self- assembling morphologies: A study of generalization via modularity. In *NeurIPS*, 2019.
- [32] C. Sferrazza, D.-M. Huang, F. Liu, J. Lee, and P. Abbeel. Body transformer: Leveraging robot embodiment for policy learning. In *Workshop on Embodiment-Aware Robot Learning*, 2024. URL <https://openreview.net/forum?id=IbXqRpANPD>.
- [33] C. Ying, T. Cai, S. Luo, S. Zheng, G. Ke, D. He, Y. Shen, and T.-Y. Liu. Do transformers really perform badly for graph representation? In *Thirty-Fifth Conference on Neural Information Processing Systems*, 2021. URL <https://openreview.net/forum?id=0eWoo0xFwDa>.
- [34] J. Schulman, F. Wolski, P. Dhariwal, A. Radford, and O. Klimov. Proximal policy optimization algorithms. *arXiv preprint arXiv:1707.06347*, 2017.
- [35] V. Makoviychuk, L. Wawrzyniak, Y. Guo, M. Lu, K. Storey, M. Macklin, D. Hoeller, N. Rudin, A. Allshire, A. Handa, and G. State. Isaac gym: High performance GPU based physics simulation for robot learning. In *Thirty-fifth Conference on Neural Information Processing Systems Datasets and Benchmarks Track (Round 2)*, 2021. URL [https://openreview.net/forum?id=fgFBtYgJQX\\_](https://openreview.net/forum?id=fgFBtYgJQX_).

## A Appendix

We provide additional details on the procedural embodiment generation (§A.1), real-world evaluations (§A.2), a forward-kinematics task (§A.3), and the GET model and training parameters (§A.4).

### A.1 Procedural Generation

In this section, we supplement the discussion in §4.1 with more details on the procedural generation of LEAP Hand embodiments. In Fig. 6 we show the diversity of zero-shot embodiments we use to evaluate GET-Zero spanning both graph and link length variations. We were able to train embodiment-specific RL experts for all 10 embodiments with graph variations (Fig. 6, row a). Doing so lets us verify that these hardware configurations are capable of completing the task with sufficient performance ( $2\pi$  rotation completed in under 30 seconds), making them reasonable targets for zero-shot generalization.

We generate the zero-shot link length extension embodiments (Fig. 6 rows b and c) by introducing link extensions to the graph variation embodiments. In particular, for row b we randomly select 10 embodiments from our set of 44 training embodiments and introduce link extensions. For row c, we use the same 10 embodiments used to evaluate zero-shot graph generalization (row a). We open source all of our code for this work on our project website, including the scripts to procedurally generate embodiments as well as the generated URDF files and assets.

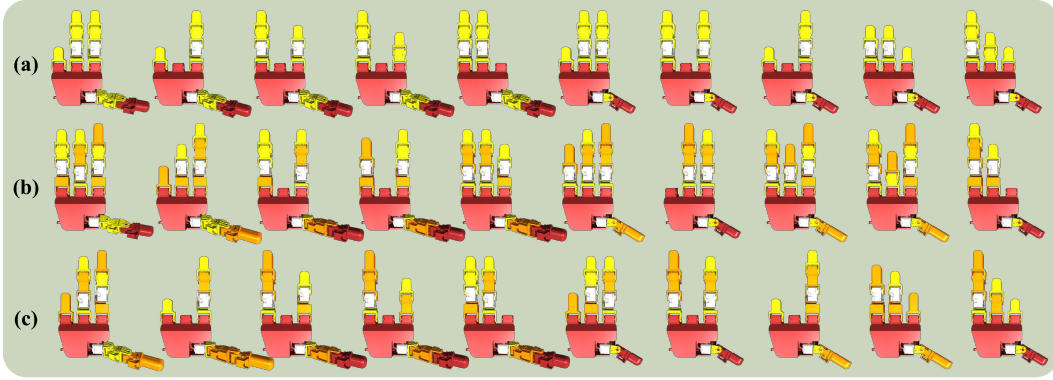


Figure 6: **Zero-shot embodiments.** We evaluate zero-shot transfer to (a) new graph variations, (b) link length extensions (orange), and (c) both link and graph variations. For each category we evaluate ten embodiments in simulation (pictured) and a subset to evaluate in real. Hands in the third row (link and graph variations) match those in the first row (connectivity variations), but with extensions applied to some links. We train on 44 hands with connectivity variations (not pictured).

### A.2 Real-world Evaluation Methodology

We conduct real world evaluation across 3 minutes of execution per embodiment and sample our GET model at 20Hz. Every 20 seconds we pause execution, automatically reset the hand to a starting pose, and manually place the cube at the center of the palm. This matches the reset procedure used in the simulation evaluations and addresses the issue where the cube could get stuck in one challenging position for the entire evaluation.

Additionally, we attach an AR tag to the top of the cube and use the RGB camera in an Intel Realsense D415 camera to track the AR tag pose to provide the rotation metric. If the cube falls off the hand, the AR tag is no longer visible and we pause execution, increment the drop counter, reset the hand pose, and reset the cube.

### A.3 Forward Kinematics Task

To further understand the self-modeling component of GET, we train a GET model with only the forward kinematics prediction head and without the action head. The main objectives are to validate 1) that the model can leverage the embodiment graph to complete a downstream task and 2) that the learned graph encoding appropriately transfers to previously unseen embodiments. We observe that GET-Zero is able to achieve much higher precision predicting the per-joint positions because of the graph encoding mechanism, which provides joint graph connectivity information that is needed to accurately compute forward kinematics (Tab. 3).

	New Graph
ET [3]	$7.97 \pm 1.36$
ET+DFS [4]	$9.03 \pm 3.22$
GET-Zero (Ours)	<b><math>0.82 \pm 0.81</math></b>

Table 3: **Zero-shot forward kinematics performance.** Measurements are a 5 seed average per-joint forward kinematics error in millimeters across 10 unseen embodiments with graph variations.

### A.4 GET Model and Training Parameters

We include the parameter choices for the GET architecture, the behavior cloning training, and the dataset in Tab. 4. We refer to Shaw et al. [8] for the embodiment-specific model architecture and training parameters used for RL experts.

	Parameter	Value
GET Model	Token dimension	512
	Token dropout	0.1
	Encoder layers	8
	Attention heads	16
	Attention dropout	0.1
	Graph embedding initialization	$\mathcal{N}(0, 0.02)$
	Feedforward dimension	1024
	Head hidden dimension	16
	Head activation	elu
Behavior Cloning	Action loss weight	1
	Self-modeling loss weight	2
	Optimizer	Adam
	Adam $\beta_1, \beta_2$	0.9, 0.98
	Epochs	7
	LR schedule	15% Linear warmup with sqrt decay
	LR max	$1.5e-4$
	Grad clip	1
Dataset	Training + sim eval time	8 hours on NVIDIA RTX A6000
	Training embodiments	44
	Train samples per embodiment	5e5
	Zero-shot embodiments (Fig. 6)	30

Table 4: **GET model, training and dataset parameters.**